Progress In Electromagnetics Research B, Vol. 78, 31–46, 2017

Measurement Methodologies for Reducing Errors in the Assessment of EMF by Exposimeter

Rodrigues Kwate Kwate[1, *], Bachir Elmagroud[1], Chakib Taybi[1], Veronique Beauvois[2], Christophe Geuzaine[2], Dominique Picard[3], and Abdelhak Ziyyat[1]

Abstract—Objective: As well known, using a single body worn sensor exposimeter introduces systematic errors on the measurement of the incident free space electric field strength. This is because the body creates around it high, intermediate and low level field zones, which depend on the direction of arrival of the incident field. The goal of this work is to propose an efficient method for the reduction of these errors. Methods: After classifying the perturbations induced by the body on the measured electric and magnetic fields thanks to realistic numerical simulations, we then propose a two-sensor setup in conjunction with simple semi-empirical correction formulas, in order to compensate these perturbations. Results: At 942 MHz, when the two sensors are placed in any opposite sides of the body at chest height, the worst case, maximum and average errors respectively decrease to 12% and 3% compared to 83% and 22% for measurement techniques using a single sensor, or 32% and 11% when using the average value of the measurements. Conclusion: The error related to the measurement in the presence of the body was significantly reduced by the proposed method making use of two opposite sensors, E-field and H-field at the chest. Significance: The conformity of exposure to EMF in terms of reference values according to the ICNIRP is given in the abscence of the human body. The interest of this work lies in the reduction of the errors made when measuring the field in the presence of the body.

1. INTRODUCTION

The International Commission on Non-Ionizing Radiation Protection (ICNIRP) [1] provides scientific advice and guidance on the health and environmental effects of non-ionizing radiation (NIR) to protect people and environment from detrimental NIR exposure. Two classes of guidance are provided, basic restrictions and reference levels. The basics restrictions use specified physical quantities (Current density and specific energy absorption rate) for directly established health effects. The references levels are provided for practical exposure assessment purposes to determine whether the basic restrictions are likely to be exceeded. All reference levels are derived from relevant basic restrictions using measurement and/or computational techniques, and some address perception and adverse indirect effects of exposure to EMF. The derived quantities are electric field strength (E), magnetic field strength (H), magnetic flux density (B) and power density (P). In any particular exposure situation, measured or calculated values of any of these quantities without body presence can be compared with the appropriate reference level. Compliance with the reference level will ensure compliance with the relevant basic restriction. In this paper, we will focus on the techniques for measuring E by radiofrequency exposimeter. Many studies also measure E or H in order to verify that the reference levels provided are not exceeded [2–9]. The ICNIRP guidelines [1] also specify that if the measured value exceeds the reference level, it does

Received 26 June 2017, Accepted 4 August 2017, Scheduled 12 August 2017

* Corresponding author: Rodrigues Kwate Kwate (r.kwatekwate@ump.ac.ma).

[1] Electronic and Systems Laboratory, Faculty of Sciences, Mohammed Premier University, Oujda, Morocco. [2] Applied and Computational Electromagnetics, Montefiore Institute, University of Liege, Belgium. [3] DRE, Signals and Systems Laboratory, CentraleSupelec, Paris, France.

not necessarily follow that the basic restriction will be exceeded. However, whenever a reference level is exceeded it is necessary to test compliance with the relevant basic restriction and to determine whether additional protective measures are necessary. Furthermore, the measurement of E is an important step which can condition the measurement of the Specific Absorption Rate (SAR) or not. Indeed, generally, it is more advisable to measure E and compare it to the reference levels in order to assess the EMF exposure. The problem about which this work is concerned comes from the fact that the measurement of E is carried out by the worn body exposimeter, whereas the reference values are given in the absence of any body. The objective of this work is to go back to the reference value of the ICNIRP from the measurement of the field in the presence of the human body.

Several studies aiming to quantify the influence of the human body on the exposimeter measurements have been published over the last decade. It is shown in [10] and [11] that the body can produce attenuations up to 30 dB at 900 MHz. The errors due to the position of the exposimeter on the body were shown to be significant in [8], with ten exposimeter positions considered (six around the waist, two on arms and two on the upper back). The study also showed the effect of frequency on the measurement error. Finally, a thorough investigation of the influence of the body for several frequency bands is presented in [9]. A number of techniques have been proposed to attenuate the EMF assessment error linked with the presence of the human body. The method proposed in [12] uses numerical simulations to estimate an average electric field and Specific Absorption Rate (SAR). The number of measurement points used in this technique is not fixed, and the method requires the knowledge of the frequency to determine the dielectric constant of each internal organ of the body before calculating the SAR. The technique cannot readily be used in practice because of the large number of sensors necessary for reliable EMF assessment. A Personal and Distributed Exposimeter (PDE) with measurements at different locations on the human body is presented in [13]. The predicted average error is 7% for 10 sensors, 13% for 3 sensors and 16% for 2 sensors. This distributed measurement approach is interesting but relies on the a priori knowledge of the ambient electromagnetic fields. Moreover, the maximum errors obtained for each combination are not reported.

Throughout this analysis, an exposimeter is materialized by a single or several sensors distributed around the human body and all connected to one processing system. Discussions will only focus on the number of sensors connected to the same processing system. The main objective of this work is to propose an efficient methods for error reducing when EMF level is to be assessed in the vicinity of human body. The following three questions are examined:

(1) What are the errors related to this assessment in the vicinity of the human body when using a single sensor exposimeter? How to qualify and quantify these errors?

(2) When several measurements sensors are used, how should they be chosen and combined? What is the impact of the number of sensors on the measurement performance? Is there an optimum number of sensors? The optimal number is the number from which the error can no longer be significantly reduced.

(3) Is it interesting to measure H in addition to E in order to evaluate EMF exposure?

This paper is organized as follows. In Section 2, we identify and classify errors due to the presence of the body. Section 3 presents error mitigation techniques. Several approaches are studied, based on distributed sensors for a single exposimeter and/or a combination of electric field and magnetic field (E, H) measurements. Two performance indicators are considered: the maximum and the average errors due to human body. A method based on a two-sensor setup in conjunction with simple semi-empirical correction formulas is recommended, as it provides a good compromise between accuracy and ease of implementation. Section 4 presents numerical and experimental results, validating the proposed methodology.

2. EXPOSURE ASSESSMENT ERRORS DUE TO BODY PROXIMITY

2.1. Electromagnetic Field around the Body

In order to define errors due to the presence of the human body, numerical simulations are performed for multiple exposure scenarios corresponding to typical situation. These are carried out with CST Studio based on finite integration technique (FIT) [14] and [15] as numerical simulation model. We

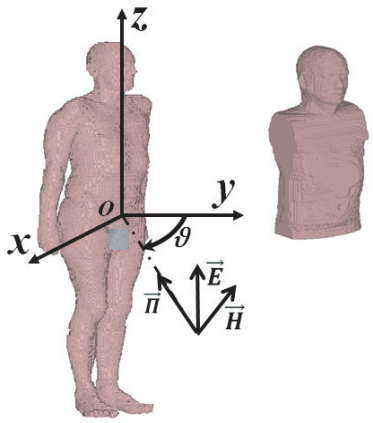

(a) (b)

Figure 1. GUSTAV human body model (from CST Studio). (a) Heterogenous whole body model. (b) Homogeneous torso model without arms.

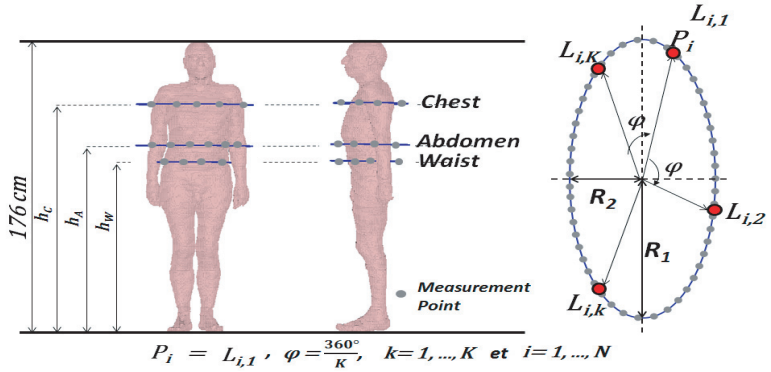

Figure 2. Locations of field evaluation points. Chest ($h_C = 143\,\text{cm}$, $R_1 = 28\,\text{cm}$, $R_2 = 17\,\text{cm}$), abdomen ($h_A = 125\,\text{cm}$, $R_1 = 28\,\text{cm}$, $R_2 = 20\,\text{cm}$) and waist ($h_W = 110\,\text{cm}$, $R_1 = 19\,\text{cm}$, $R_2 = 18\,\text{cm}$); $\widehat{L_{i,k}L_{i,k+1}} = \widehat{L_{i,k}L_{i,1}} = \varphi$ (Angle between two consecutive points used for field measurement) ; R_1 and R_2 are respectively the major and minor radii of ellipses defined for each measurement height.

use the heterogeneous human body model [16] (GUSTAV, man, 176 cm, 69 kg, 38 years): see Figure 1 (Page 3). The exposure consists in a plane wave with $1\,\text{Vm}^{-1}$ electric field. The magnitudes of the electromagnetic fields (E_{P_i} and H_{P_i}) are evaluated on N points P_i ($i = 1, \ldots, N$) located on ellipses around the body, at three different heights — around the chest, abdomen and waist (see Figure 2). These fields are provided by CST studio.

2.2. Error Definitions

Let $E_{P_i}^{\text{body}}$ denote the strength of the electric field at point P_i with the presence of body and $E_{P_i}^{\text{free}}$ the undisturbed electric field strength at the same point in the absence of human body as recommended by the ICNIRP [1]. Indeed, the strength of the electric field is measured in free space at a given location which will then be compared to the reference levels in order to check compliance with standards. Figure 3 shows three major zones in each incident field scenario:

- The zone where the E-field is greater than the incident one for vertical and horizontal polarizations. This is the reflection zone $S_R = \{P_i : E_{P_i}^{\text{body}} > E_{P_i}^{\text{free}}\}$. We donote by N_R the number of points in this zone, in which we will define a *Body Reflection Error* (BRE).
- The zone where the E-field in the presence of the body is less than 30% of the free space field. These

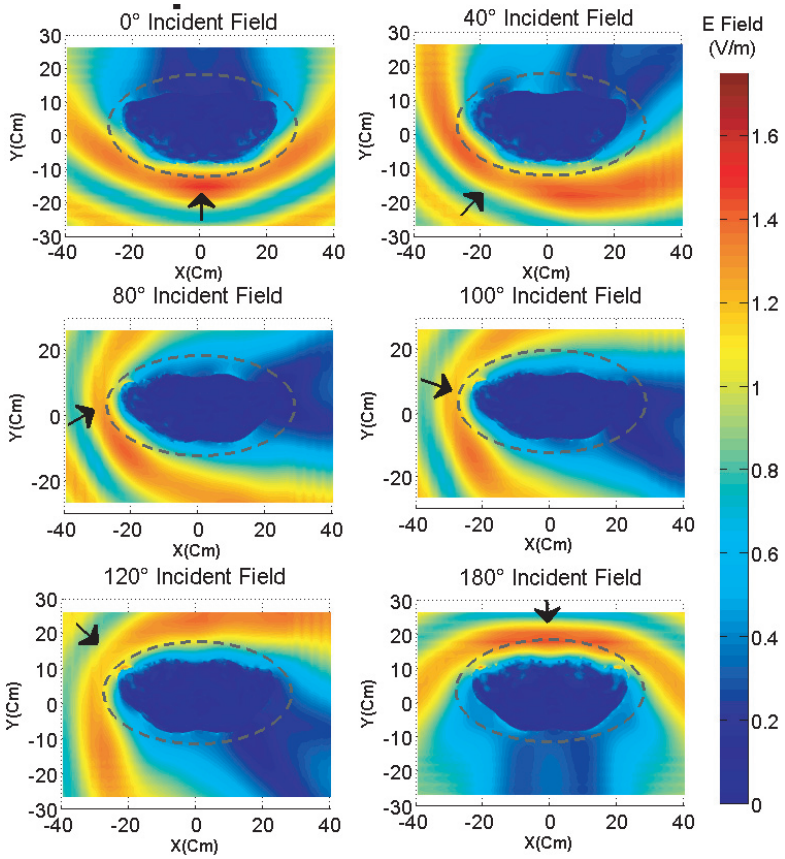

Figure 3. Electric field strength at chest height. The arrow represents the incident field direction (with vertical polarization).

values represent the measurement points in the shadowing zone $S_S = \{P_i : E_{P_i}^{\text{body}} < 0.3E_{P_i}^{\text{free}}\}$. We denote by N_S the number of points in this zone, in which we define a *Body Shadowing Error* (BSE). This error is the most important one when using an exposimeter to evaluate the EMF. Some work has already tried to quantify this error [2, 3].

- Between the two previous zones, the diffraction zone $S_D = \{P_i : 0.3.E_{P_i}^{\text{free}} \leq E_{P_i}^{\text{body}} \leq E_{P_i}^{\text{free}}\}$. We denote by N_D the number of points in this zone, in which we define *Body Diffraction Error* (BDE).

The errors in the different zones are defined as follows:

$$\text{BRE} = \frac{100}{N_R} \sum_{P_i \in S_R} \frac{E_{P_i}^{\text{free}} - E_{P_i}^{\text{body}}}{E_{P_i}^{\text{free}}} \tag{1}$$

$$\text{BSE} = \frac{100}{N_S} \sum_{P_i \in S_S} \frac{E_{P_i}^{\text{free}} - E_{P_i}^{\text{body}}}{E_{P_i}^{\text{free}}} \tag{2}$$

$$\text{BDE} = \frac{100}{N_D} \sum_{P_i \in S_D} \frac{E_{P_i}^{\text{free}} - E_{P_i}^{\text{body}}}{E_{P_i}^{\text{free}}} \tag{3}$$

In addition to these zone errors, we define a *Body Depolarization average Error* (BPE), which quantifies the depolarization due to the body. If the incident field is polarized vertically, we define

$$\text{BPE}_H = \frac{100}{N} \sum_{i=1}^{N} \frac{E_{H,P_i}^{\text{body}}}{E_{P_i}^{\text{free}}}, \tag{4}$$

where $E_{H,P_i}^{\text{body}} = \sqrt{E_{x,P_i}^{\text{body}^2} + E_{y,P_i}^{\text{body}^2}}$, and N, used in Equations (4), (5) and (6), is the variable of number of points in which strength of field is evaluated, as mentioned on this page, at the beginning of first column. If the incident field is polarized horizontally, we define

$$\text{BPE}_V = \frac{100}{N} \sum_{i=1}^{N} \frac{E_{\perp,P_i}^{\text{body}}}{E_{P_i}^{\text{free}}}, \tag{5}$$

where $E_{\perp,P_i}^{\text{body}}$ is the field in the plane orthogonal to the incident polarization. Finally, we define the *Body average Error* (BE) as follows:

$$\text{BE} = \frac{100}{N} \sum_{i=1}^{N} \frac{E_{P_i}^{\text{free}} - E_{P_i}^{\text{body}}}{E_{P_i}^{\text{free}}} \tag{6}$$

In addition to these average errors, we will also report the maximum, pointwise errors that are obtained with each of the proposed methods. Indeed, the determination of the electric field strength with precision will make it possible in practice to compare it with the reference values, in order to verify compliance with standards that regulate people's exposure to electromagnetics fields.

3. ERROR MITIGATION TECHNIQUES

We propose two families of error mitigation techniques:

3.1. Multi-Coefficient Method

The multi-coefficient method is based on multiple linear regression analysis, which attempts to model the relationship between two or more explanatory variables and a response variable by fitting a linear equation to observed data. Here, we look for a relation between the values measured in the presence of human body and the values measured in free space. To obtain this relation, it is necessary to determine the regression coefficients (vector A) that minimize the residual (vector R^a). For each situation, the vector A is obtained based on the numerical calculations carried out by the codes that we have written with Matlab:

$$E^{\text{free}} = X^{\text{body}} A + R^a, \tag{7}$$

with

$$E^{\text{free}} = \begin{matrix} 1 \\ \vdots \\ i \\ \vdots \\ N \end{matrix} \begin{pmatrix} E_{P_1}^{\text{free}} \\ \vdots \\ E_{P_i}^{\text{free}} \\ \vdots \\ E_{P_N}^{\text{free}} \end{pmatrix}; \quad A = \begin{matrix} 1 \\ \vdots \\ k \\ \vdots \\ K \end{matrix} \begin{pmatrix} a_1 \\ \vdots \\ a_k \\ \vdots \\ a_K \end{pmatrix}. \tag{8}$$

The X^{body} matrix is composed by N rows and K columns. The different methods are based on the possibility of measuring four different quantities, all in V/m. For any (i,k) position on the measuring ellipse (Figure 2), we can measure, $V1_{L_{i,k}}^{\text{body}} = E_{L_{i,k}}^{\text{body}}$, $V2_{L_{i,k}}^{\text{body}} = Z_0 \times H_{L_{i,k}}^{\text{body}}$, $V3_{L_{i,k}}^{\text{body}} = \max(E_{L_{i,k}}^{\text{body}}, Z_0 \times H_{L_{i,k}}^{\text{body}})$ and $V4_{L_{i,k}}^{\text{body}} = (E_{L_{i,k}}^{\text{body}} + Z_0 \times H_{L_{i,k}}^{\text{body}})/2$. So, the (i,k) entry $x_{L_{i,k}}^{\text{body}}$ in this matrix is defined as:

$$x_{L_{i,k}}^{\text{body}} = \begin{cases} V1_{L_{i,k}}^{\text{body}} & \text{[M11]} \\ V2_{L_{i,k}}^{\text{body}} & \text{[M12]} \\ V3_{L_{i,k}}^{\text{body}} & \text{[M13]} \\ V4_{L_{i,k}}^{\text{body}} & \text{[M14]} \end{cases} \tag{9}$$

where $Z_0 \approx 120 \times \pi \approx 376.99\,\Omega$ is the wave-impedance of a plane wave in free space, and $E^{\text{body}}_{L_{i,k}}$ and $H^{\text{body}}_{L_{i,k}}$ are respectively the electric field strength and the magnetic field strength measured at the $L_{i,k}$ position on the body. M11, M12, M13 and M14 denote the different ways to consider $x^{body}_{L_{i,k}}$ in the multi-coefficient method.

The residual vector R^a contains the N errors terms: the maximum error is $R^a_{\max} = \max(R^a_i)$, and the average error is $R^a_{\text{mean}} = \text{mean}(R^a_i)$, $i = 1, \ldots, N$.

3.2. Single-Coefficient Method with Maximum Value

The single-coefficient method is based on a simple linear regression:

$$E^{\text{free}} = b\, Y^{\text{body}} + R^b \tag{10}$$

where b is the single correction factor and where the i-th entry $y^{\text{body}}_{P_i}$ in the vector Y^{body} is defined as:

$$y^{\text{body}}_{P_i} = \begin{cases} \max(V1^{\text{body}}_{L_{i,1}}, ..., V1^{\text{body}}_{L_{i,K}}) & \text{[M21]} \\ \max(V2^{\text{body}}_{L_{i,1}}, ..., V2^{\text{body}}_{L_{i,K}}) & \text{[M22]} \\ \max(V3^{\text{body}}_{L_{i,1}}, ..., V3^{\text{body}}_{L_{i,K}}) & \text{[M23]} \\ \max(V4^{\text{body}}_{L_{i,1}}, ..., V4^{\text{body}}_{L_{i,K}}) & \text{[M24]} \end{cases} \tag{11}$$

In this method, we take maximum quantity for all the K points used in measuring ellipse. The residual vector R^b contains the N error terms. As for the multi-coefficient method, the maximum error is $R^b_{\max} = \max(R^b)$, and average error is $R^b_{\text{mean}} = \text{mean}(R^b)$. M21, M22, M23 and M24 denote the different ways to consider y^{body} in the single-coefficient method.

In addition to the eight methods described above, we also consider method M00, which represents a conventional measurement technique using a single sensor, as well as methods M10 and M20, which represent the simple cases when we just measure the electric field in a two-sensor setup, either by averaging the values (M10) or taking the maximum value (M20). M10 is also used in [13].

4. RESULTS AND DISCUSSION

4.1. Comparison between Simulations and Measurements

To validate the simulations, measurements have been carried out at 900 MHz in a full anechoic room with vertical and horizontal polarizations, and the level of the reflected waves on the walls of the chamber is approximately -50 dB (0.3% in magnitude). A SATIMO dual-ridge 600 MHz–9 GHz horn antenna is used to produce the incident field (Figure 4), and a wideband probe (En-Probe EFS-105, 5 MHz–3 GHz with noise $< 10\,\mu\text{V} \cdot \text{m}^{-1}\text{Hz}^{-1/2}$ from 200 to 500 MHz and $< 30\,\mu\text{V} \cdot \text{m}^{-1}$ from 500 MHz to 3 GHz) is used as an exposimeter. This probe is connected to the base unit through an optical fiber link, and the base unit is connected to a network analyzer (VNA, Agilent ENA 5071b) through a short cable. The exposimeter is placed at 3 cm of the surface of the human body model. The human body model is filled by a fluid with relative permitivity 60 and conductivity $1.2\,\text{Sm}^{-1}$ as recommended by Federal Communication Commission (FCC) in the report entitled, evaluating compliance with FCC guidelines for human exposure to radiofrequency electromagnetic fields. The body model turns on itself following the angle ϑ ($-\pi \leq \vartheta \leq \pi$) and is placed in the far field region (472 cm) of the antenna. This movement system is managed by a motor programmed for this purpose. All measurements are made by cycles. A measuring cycle is characterized by the fact that the entire system (human body and probe) performs a rotational movement on itself of $-\pi \leq \vartheta \leq \pi$ with an angle $\pi/4(45°)$ of increment. Another cycle will be defined by another position of a probe on the human body at the same height but at an angular deviation of $2\pi/9$ also. For example, a cycle can be performed with a probe at 0° in the torso as in Figure 4, and another cycle will be done for the probe at pi. Figure 5 compares measured and simulated values around the body: a good match is observed, with a relative root mean square deviation of 14% and maximum relative deviation is 40%.

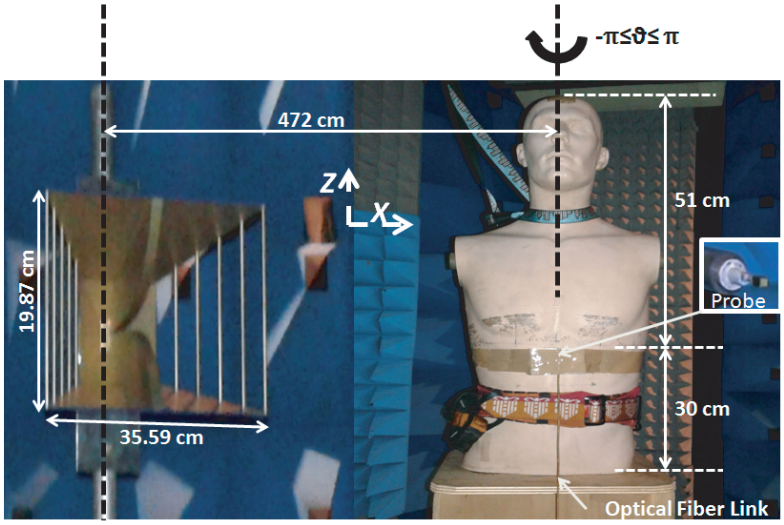

Figure 4. Measurement validation tools: antenna, probe and human body model.

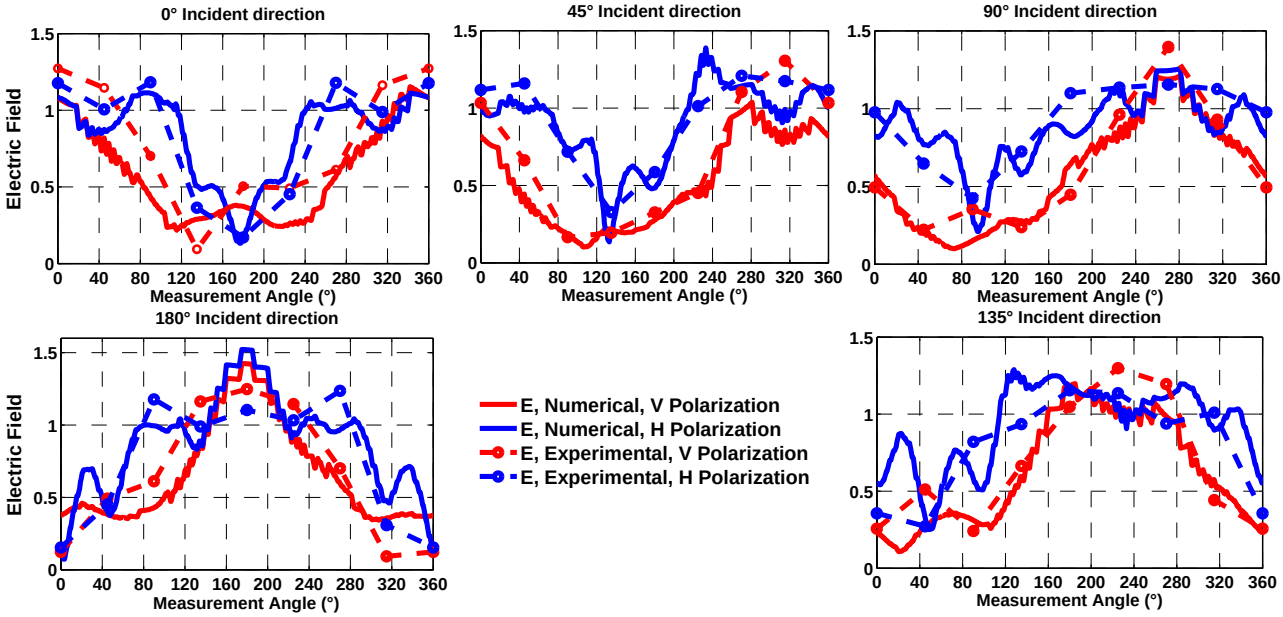

Figure 5. Comparison between measurements and simulations at 942 MHz.

4.2. Body Errors Classification for a Single Point

The variation of the intensity of the electric (E) and magnetic (H) fields along the axis OY at height $z = h_c$ is shown in Figure 6. The intensity of the electric field varies from 0.51 V/m on the surface of the human body, to 1.47 V/m at 17.4 cm distance from the surface of the body. The intensity of the magnetic field changes from 3.93 10^{-3} A/m at the surface of the human body to 1.26 10^{-3} A/m for the vertical polarization at 400 MHz. This distance of 17.4 cm is equivalent to the quarter of the wavelength for a frequency of 400 MHz. For the frequencies 942 MHz and 1842 MHz, we also make the same observation. We deduce that whatever the polarization of the incident field, opposite to the direction of arrival of the incident field and with the presence of the human body, maximum of the electric field strength coincides with minimum of the magnetic field strength and vice versa.

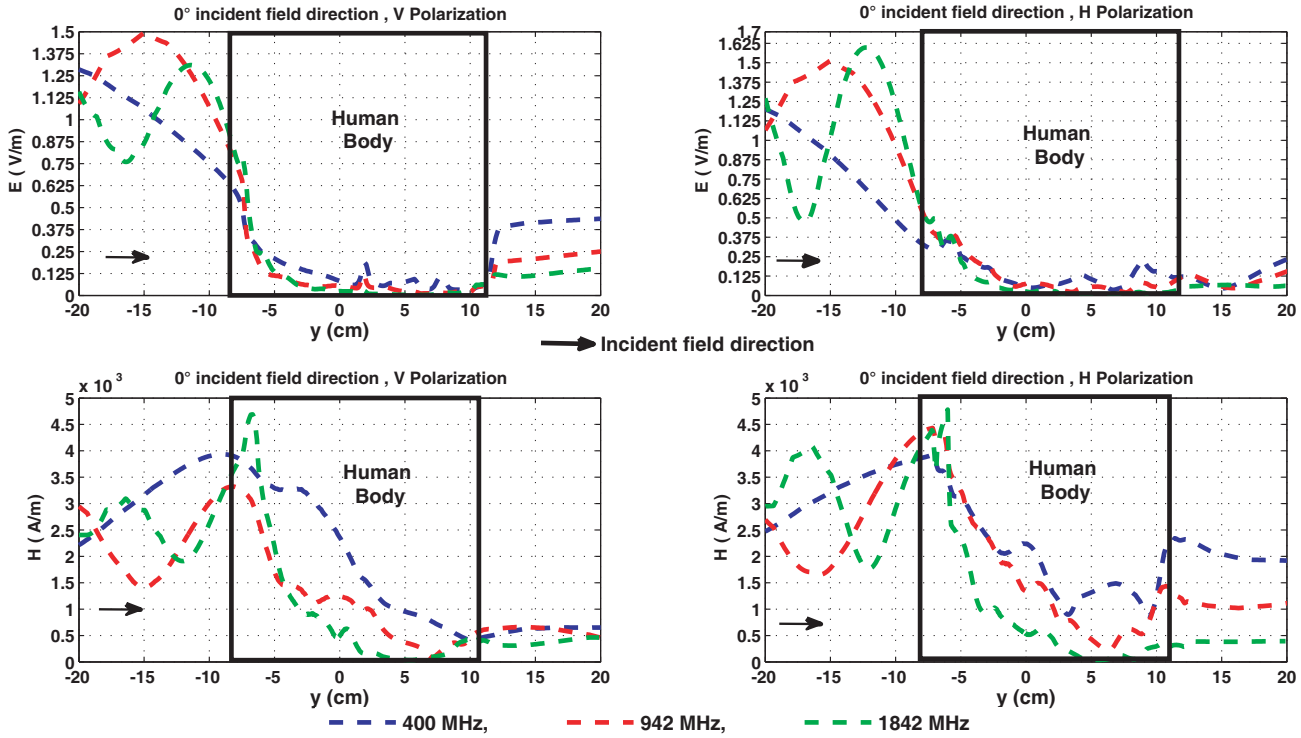

Figure 6. Variation of E and H fields along the OY axis at height $z = h_c = 143\,\text{cm}$ with the presence of human body. For 400 MHz, 942 MHz and 1842 MHz.

This observation can also be made with the measuring ellipse in the direction of arrival of the field or reflection zone (Figure 7). These remarks allow us to imagine that an exposimeter worn on the front and capable of simultaneously measuring both electric and magnetic components will be less susceptible to under-estimating the incident field strength (when arriving from the front) due to a null in one of the components caused by destructive interference. However, an under-estimation in both components of the field cannot be avoided when an exposimeter is located at the rear where the body shields the exposimeter from the front incident plan wave. Overall, similar variability in the electric and magnetic field strengths close to the body is observe.

We classify assessment errors due to the presence of the body and present an assessment based on the combination approach (distributed measurements, electric and magnetic fields). As shown in [10, 11] and [17–19], using a single sensor is largely ineffective in an overall estimation exposure. Indeed, Figures 3 and 7 show the field level around the chest for different incident fields direction. Particularly in Figure 7, we compare four fields quantities with the incident field in free space such as: E-field with body presence $V1^{\text{body}}$, $V2^{\text{body}}$, $V3^{\text{body}}$ and $V4^{\text{body}}$. This shows how $V1^{\text{body}}$ and $V3^{\text{body}}$ curves match for on all diagrams, and there is noticeable difference between $V2^{\text{body}}$, $V4^{\text{body}}$ and $V1^{\text{body}}$ curves, in central parts of diagrams regarding direction of arrival of incident field. This can be explained by the result obtained in Figure 6. Indeed, at a distance from the human body less than a quarter of the wavelength of the incident field (7.75 cm for 942 MHz), opposite to the direction of arrival of the incident field, $V1^{\text{body}} \approx V3^{\text{body}} \approx \max(E^{\text{body}}, Z_0 H^{\text{body}})$ because $E^{\text{body}} > Z_0 H^{\text{body}}$, and at the rear side (back) of the human body relative to direction of arrival, E^{body} and $Z_0 H^{\text{body}}$ are both very low. On the other hand, it can be seen that the two fields E and $Z_0 \times H$ act in a complementary manner around the reference value, hence the interest to study the measured values as the average defined by $(E + Z_0 \times H)/2$. Relative to this observations, a measurement method based on multiple points distributed in the reflection, diffraction and shading zones is required.

As shown in Figure 9 (Page 9) and Figure 10 (Page 9), we present assessment errors due to the presence of the human body as a boxplot. In descriptive statistics, a boxplot is a convenient way of

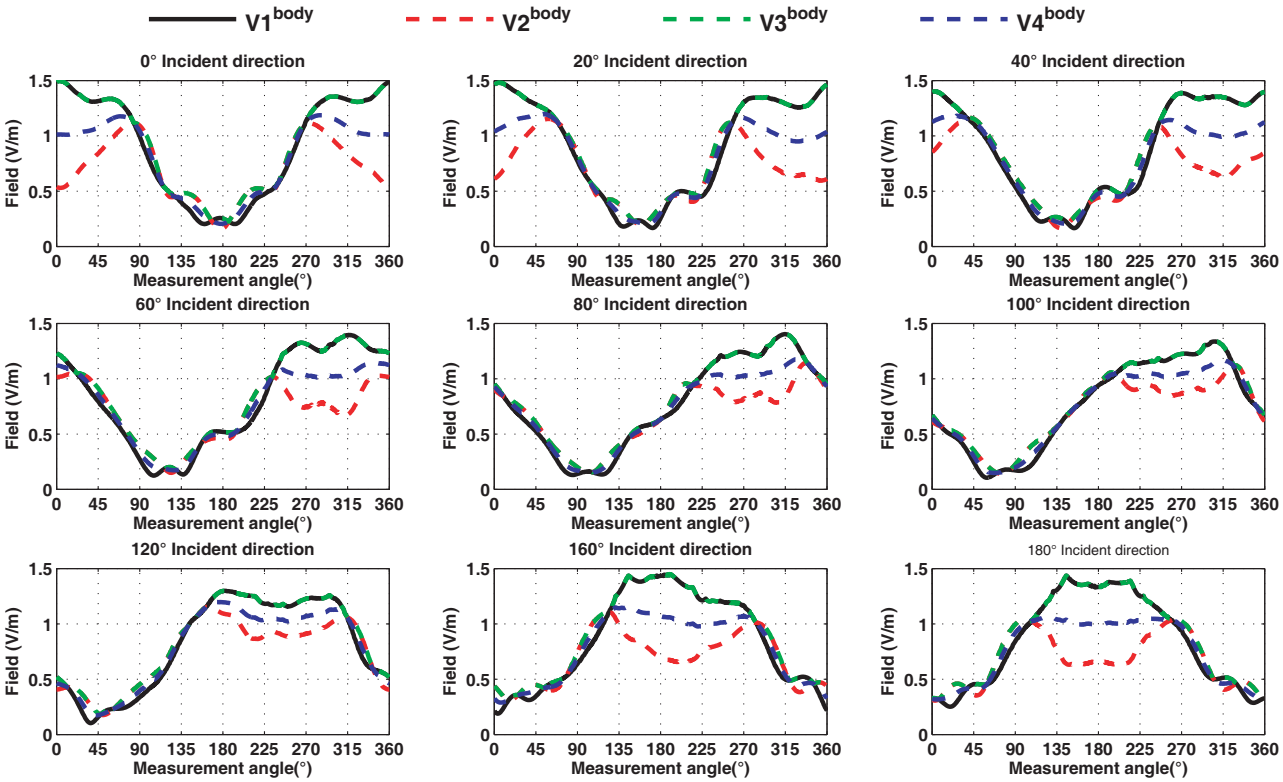

Figure 7. Elliptical scanning at chest height of the human body (Vertical polarization, 942 MHz).

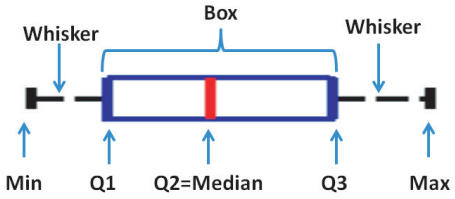

Figure 8. BoxPlot explanation.

graphically depicting groups of numerical data through their quartiles. The boxplot (Figure 8, Page 8) displays the distribution of data based on the five-number summary: minimum (Min), first quartile (Q_1), median (Q_2), third quartile (Q_3), and maximum (Max). The median is the number that divides the studied data into two groups containing the same number of elements. This parameter is useful to give the distribution of the character studied, because about 50% of the data studied has a modality lower than the median and 50% a modality higher than the median. The spacings between different parts of the box indicate the degree of dispersion (spread) and skewness in the data. A segment inside the box shows the median, and whiskers above (25% of datas) and below (25% of datas) the box show the locations of the minimum and maximum. Not uncommonly real data-sets will display surprisingly high maximums or surprisingly low minimums called outliers. Following this study, we will call $IQ = [Q_1, Q_3]$ the interquartile interval (50% of datas); its range will be calculated as $IQR = ||Q_3| - |Q_1||$. The variation range for each error data type will also be investigated and calculated as $\Delta = ||\text{Max}| - |\text{Min}||$. As we study the behavior of the EMF in the vicinity of the human body in order to use this knowledge to better evaluate the field in free space, we will use the statistical variables defined above for the study of this behavior. The values IQR and Δ inform us about the degree of convergence of the data with respect to the median value of the errors that each method can produce. The maximum (Max) error is also important because it tells us on the ceiling that we can reach. Moreover, the statistical study also

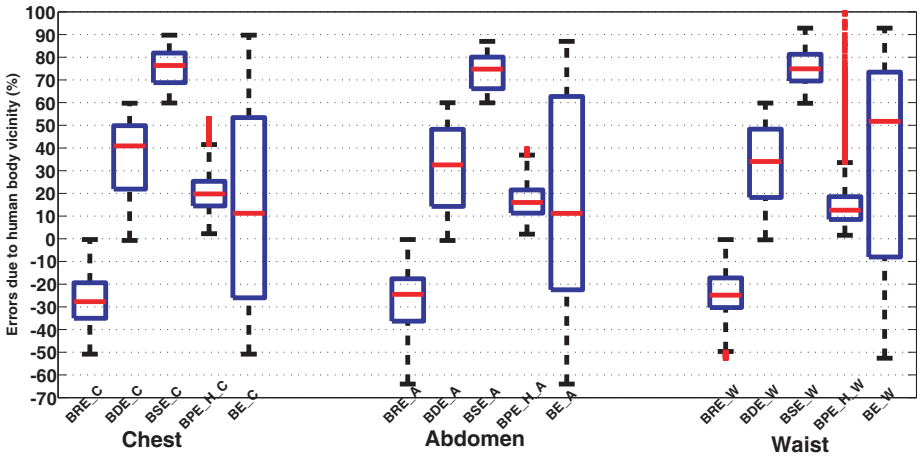

Figure 9. Assessment Errors due to proximity of the Body (Vertical polarization).

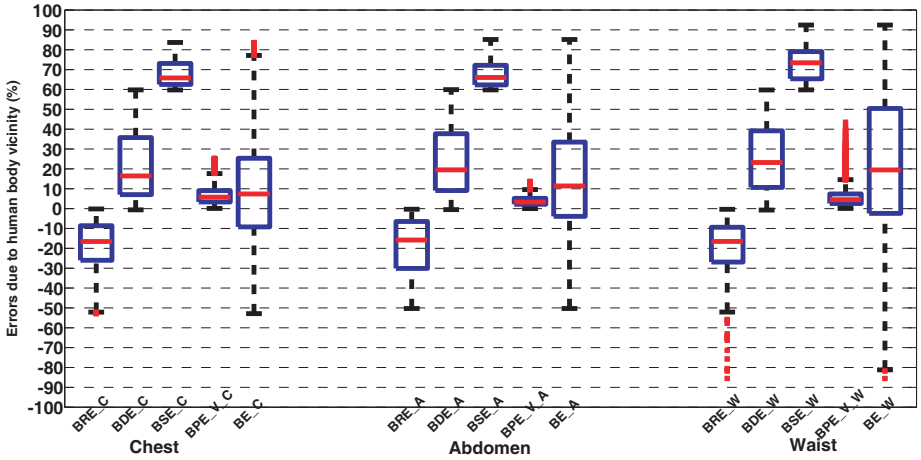

Figure 10. Assessment Errors due to proximity of Body (Horizontal polarization).

gives the behavior of all the situations, hence the values of interest such as IQR and Δ.

Figures 9 and 10 show that the human body barely depolarizes the incident field. Indeed, the boxplot representing the depolarization error (BPE_V when the incident field is horizontally polarized and BPE_H when the incident field is vertically polarized) has a median less than 20% for the BPE_H and 10% for the BPE_V. The IQR of depolarization varies between 3% and 11%, which reflects the fact that the values of BPE_H and BPE_V are very close to the median. It means that it will be more obvious to find suitable weighting coefficients to mitigate the error due to depolarization. The errors due to depolarization are lower than other errors (BRE, BDE, BSE and BE), but their values are not negligible and will be specifically treated later. Overall, for a given incident polarization, it would be better to measure the same polarization close to the human body. These are the same points that we can do regarding the errors due to the mask (BSE), with the following features: IQR between 10% and 14% and the maximum difference between the errors due to the human body mask (Δ) varies in each case between 24% and 33%. Whatever the polarization of the incident field and the measurement level (Chest, waist and abdomen), the errors due to the measurement in the mask zone (BSE) is between 80% and 99% relative to the electric field level measured at the same place in free space (without the presence of the human body). In sum, the errors due to the mask areas are the most important ones that require a large correction, and these errors also have the particularity of being grouped around the median value.

We also notice that errors due to reflection of the incident field by the body are mostly overestimated. Indeed, the boxplots representing all the BRE are mostly in the negative part of the graph. Moreover, their IQR between 13% and 24% means that nearly 50% of the measured samples are quite close within 25% of their median value, the median value that varies between 15% and 27% (i.e., between 1.15 V/m and 1.27 V/m). In other words, in vertical polarization, half of the measurements made in the reflection zone is between 1 V/m and 1.15 V/m, and the other half is more than 1.15 V/m. In horizontal polarization, half of the measurements made in the reflection zone is between 1 V/m and 1.27 V/m, and the other half is more than 1.27 V/m. The maximum difference between the errors due to the reflection of the incident field by the human body (Δ) is between 0% and 63% (between 1 V/m and 1.63 V/m) and particularly between 0% and 85% (between 1 V/m and 1.85 V/m) for horizontal polarization and for measurements made at the waist level. In terms of outliers, we notice that they are usually present when it comes to make measurements in the waist zone. This is due to the presence of the arms in this region. Indeed, when we approach the zone of the chest, this is reduced considerably; it can also be noticed that, as we presented in [19], the chest zone is the most stable zone and most recommended for assessment of personal body exposure. On the other hand, while making these remarks, the outliers do not represent more than 6% (BPE_V_W horizontal polarization) of all the measurements carried out. This reflects the fact that the data are quite clustered in the boxplot.

4.3. Error Mitigation Results

For K measurement points ($\phi = 360°/K$), we show in Figure 11 how the average error (BE) decreases with the increase of the number of points (K). This extends the results that we presented in [19] and [20] for two measurement points. When the number of measuring points increases, it is possible to get at least one point in the reflection or diffraction zones, and the average of measurements will be closer to the free space value of the field: for chest height and vertical polarization, we have $IQR = 30\%$ and $\Delta = 89\%$ for a single point, $IQR = 12\%$ and $\Delta = 36\%$ for 2 points, $IQR = 11\%$ and $\Delta = 28\%$ for 3 points and $IQR = 8\%$ and $\Delta = 28\%$ for 4 points. In other words, after three points or sensors, it is no longer necessary to increase the sensors because the impact on the performance of the measurement is no longer very significant. These observations are also clearly shown in Tables 1 and 2 and Figure 12. Indeed, with the method that we propose (M24), we obtain the best error reduction for only two measurement

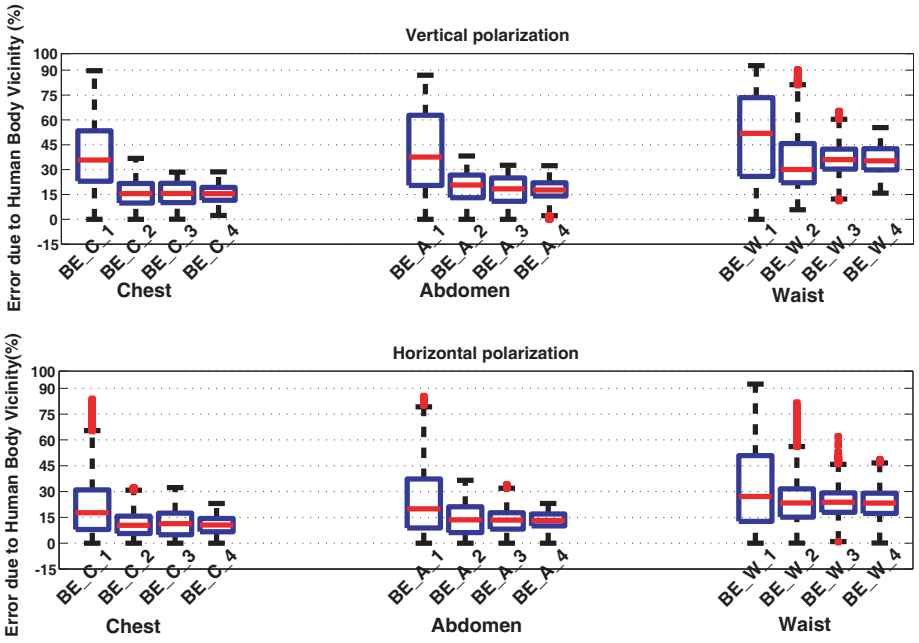

Figure 11. Assessment errors based on simultaneously K measurements points, average combination. $K = 1, 2, 3$ or 4.

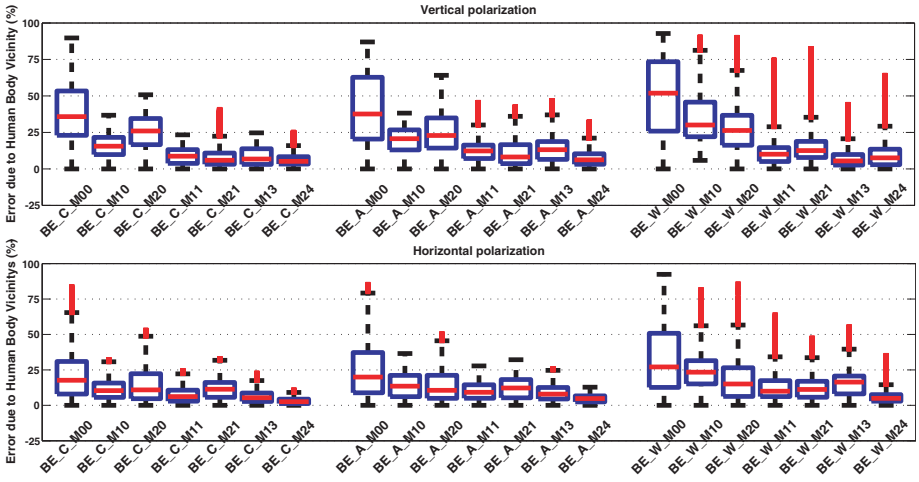

Figure 12. Comparison between the assessment errors obtained for the different techniques M00 (BE_M00), M10 (BE_M10), M20 (BE_M20), M11 (BE_M11), M21 (BE_M21), M13 (BE_M13) and M24 (BE_M24).

points (Reduction of 8 times in terms of average error and 3 to 7 times in terms of maximum error). We also note that, for a single E-field sensor, regardless of the measurement level (chest, abdomen and waist), the behaviors of average and maximum errors are the same. For conventional measurement methods with two E-field sensors, M10 (average method) and M20 (maximum method) are described in the last paragraph of Section 3.2 (Single-coefficient Method with Maximum Value).

It is necessary to avoid making measurements at the waist level, because it presents twice as many errors as the other positions (Chest and abdomen) with a slight preference for chest level. The robustness of M24 method compared to others is due to the combination of E-field and H-field with two points diametrically opposed to the measuring ellipse. This result considerably reduces the complexity of the exposimeter presented in [13]. Several exposimeters as ESM-30 RADMAN XT already measure the electric and magnetic fields. By combining two sensors of this exposimeter with the M24 method, we will get 3% average error and 12% maximum error in free space electric field strength assessment.

Table 1. Correction parameters for vertical polarization and two measurement points.

			Multi-coefficient method						Single-coefficient method				
		M00	M10	M11	M12	M13	M14		M20	M21	M22	M23	M24
Chest	a_1	-	0.5	0.58	0.67	0.56	0.63	b	1	0.80	1.09	0.79	0.94
	a_2	-	0.5	0.58	0.67	0.56	0.63						
	$R^a_{\text{mean}}(\%)$	39	15	8.44	20.8	8.21	12.4	$R^b_{\text{mean}}(\%)$	25	9.30	14.3	8.55	5.36
	$R^a_{\text{max}}(\%)$	89	36	25.8	53.0	26.4	37.3	$R^b_{\text{max}}(\%)$	50	39.6	41.9	33.3	24.6
Abdomen	a_1	-	0.5	0.59	0.66	0.56	0.63	b	1	0.80	1.03	0.80	0.92
	a_2	-	0.5	0.59	0.66	0.56	0.63						
	$R^a_{\text{mean}}(\%)$	41	19	12.0	21.2	13.4	14.5	$R^b_{\text{mean}}(\%)$	24	11.09	11.6	10.2	7.58
	$R^a_{\text{max}}(\%)$	86	38	45.4	58.2	46.8	52.9	$R^b_{\text{max}}(\%)$	63	42.5	48.5	39.2	32.1
Waist	a_1	-	0.5	0.72	0.78	0.67	0.77	b	1	0.91	1.09	0.88	1.02
	a_2	-	0.5	0.72	0.78	0.67	0.77						
	$R^a_{\text{mean}}(\%)$	49	36	20.6	20.1	13.3	14.8	$R^b_{\text{mean}}(\%)$	28	26.0	15.9	17.5	16.4
	$R^a_{\text{max}}(\%)$	90	89	85.5	76.3	62.8	65.3	$R^b_{\text{max}}(\%)$	89	90.5	83.0	73.3	76.5

Table 2. Correction parameters for horizontal polarization and two measurement points.

			Multi-coefficient method						Single-coefficient method				
		M00	M10	M11	M12	M13	M14		M20	M21	M22	M23	M24
Chest	a_1	-	0.5	0.55	0.62	0.53	0.59	b	1	0.89	1.1	0.87	1.01
	a_2	-	0.5	0.55	0.62	0.53	0.59						
	$R^a_{\text{mean}}(\%)$	22	11	7.23	19.12	6.77	10.77	$R^b_{\text{mean}}(\%)$	13	11.2	14.4	8.78	3.31
	$R^a_{\max}(\%)$	83	32	24.7	50.2	21.2	25.1	$R^b_{\max}(\%)$	52	36.4	38.1	33.7	12.2
Abdomen	a_1	-	0.5	0.57	0.63	0.54	0.60	b	1	0.90	1.04	0.87	1.00
	a_2	-	0.5	0.57	0.63	0.54	0.60						
	$R^a_{\text{mean}}(\%)$	24	14	9.21	15.27	7.83	8.78	$R^b_{\text{mean}}(\%)$	14	13.6	12.77	10.5	4.97
	$R^a_{\max}(\%)$	82	36	27.5	49.7	25.8	20.9	$R^b_{\max}(\%)$	50	35.5	45.3	30.2	14.7
Waist	a_1	-	0.5	0.62	0.62	0.55	0.63	b	1	0.94	0.93	0.84	0.98
	a_2	-	0.5	0.62	0.62	0.55	0.63						
	$R^a_{\text{mean}}(\%)$	32	24	15.4	20.7	14.2	15.7	$R^b_{\text{mean}}(\%)$	17	16.8	17.9	11.3	7.53
	$R^a_{\max}(\%)$	92	79	75.0	61.9	59.9	54.3	$R^b_{\max}(\%)$	81	78.0	52.4	52.0	43.9

We also show through Tables 1 and 2 that regardless of polarization, the conventional single E-field sensor method produces the same errors, and the proposed method reduces the average error (8 times) in the same way as that in the presence of a horizontally or vertically polarized incident field. However, this method (M24) is more efficient in terms of maximum error reduction for horizontal polarization (7 times) than for vertical polarization (3 times). Finally, our study shows that with conventional methods, the use of the average (M10) or the maximum value (M20) of the E-field measured in the vicinity of human body by multiple sensors reduces 2 times of the errors compared to M00 method that uses a single E-field sensor. Moreover, a much better correction is observed with the method of the average (M10) than with that of the maximum (M20). However, with the methods that we propose, if we can just measure the E-field at two diametrically opposed points (Method M11), then the maximum and average errors are reduced 4 times, respectively to 26% and 8% compared to 89% and 39% for method M00. In this study, a much better method is also proposed combining the simultaneous measurement of E and H fields at two diametrically opposed points (M24). Indeed, if we have this possibility, the average error is reduced 8 times (39% to 5%) regardless of the polarization of the incident field. The maximum error is also reduced 3 times (89% to 24%) for vertical polarization and 7 times (83% to 23%) for horizontal polarization compared to the conventional method.

The contribution of the work presented in this paper can be evaluated in relation to some recent works carried out in the bibliography on the same thematic [2–4]. Indeed, to study the potential errors associated with the exposure measurements to non-ionizing radiations due to the influence of the BSE (Body Shadow Effect/Error) in order to quantify that influence, the assessment of human body influence on exposure measurements of electric field in indoor enclosures [2] and the analysis of polarization dependence of BSE on dosimetry measurements in 2.4 GHz band [3] have recently been treated. We note that these works focus mainly and exclusively on the error due to shadowing phenomenon. Moreover, in this paper we show the importance of also taking into account the error due to the reflection or the diffraction of the incident electromagnetic field on the human body. The study presented in [2], like this paper, demonstrates that if we do not consider BSE (Body Shadow Error) in the exposure assessment, then it will translate into measurement by underestimating the exposure to which the human body is effectively subjected. We have used these remarks to propose new methods for measuring the electric field by an exposimeter in order to compare them to the reference values. In the same order of ideas, the study of the role of the location of personal exposimeters on the human body in their use for assessing exposure to the electromagnetic field in the radiofrequency range 98 to 2450 MHz and compliance analysis (evaluation by numericals simulations) is done [4]. Using the Gustav model as a numerical model of the human body, measurements are made in 4 locations (front, right, left and back) at each level (Chest and waist). In an environmental test regarding compliance with the

binding requirements, the study proposes to use a correction factor (applied to the measurement results or alternatively to the exposure limit values) to compensate such discrepancies between the result of an exposimetric measurement and the exposure metric expected by the exposure limit provider (such as international organization or national legislator). The solution with only one measurement location or sensor can be interesting, but the correction factor will depend on the position of the exposimeter and the parameters that we do not master as the direction of arrival of the field. Moreover, we propose to combine two diametrically opposite points measurements before applying the correction by factors, which give us the assurance that at least one of the two measurement points will always be in the reflection or diffraction zone of the field on the human body whatever the direction of arrival. Although in future work we will perform the same analysis for a wide range of frequencies, we can say that the current studies on the frequencies DCS 1842 MHz and LTE/Wimax 3500 MHz show similar results to those of 942 MHz presented in this work.

5. CONCLUSION

In this work, according to ICNIRP, the error considered is the difference between the field value measured by an exposimeter in the presence of the body and the field value in its absence. In the method proposed by this work, we have reduced this error by 8 times compared to the conventional method. This good result is achieved with the following results:

- ***Sensor(s) location***: Whatever the method used, it is necessary to avoid making measurements at the waist level which presents far more errors than chest and abdomen levels, with a slight preference for chest.
- ***Sensors number***: With method M24, we obtain the best error reduction for only two measurement points. After three measurements sensors, it is no longer necessary to increase the number of sensors because the impact is no longer very significant.
- ***Incident field polarization***: Regardless of the polarization, the proposed method (M24) reduces the average error by 8 times. Method M24 is more efficient in terms of maximum error reduction for horizontal polarization (7 times) than for vertical polarization (3 times).
- ***Measurement methodologies***: Conventional two-sensor setup methods reduce the errors by 2 times. However, with our methods, if we can just measure the E-field at two diametrically opposed points, then the maximum and average errors are reduced 4 times compared to the conventional single sensor method. A much better method is also proposed combining the measurement of E-field and H-field. In that case, the average error is reduced 8 times regardless of the polarization. The maximum error is also reduced 8 times for horizontal polarization but just 3 times for vertical polarization.

Future work will consider a greater range of frequencies, other human body models morphologies and other exposure situations.

ACKNOWLEDGMENT

This work is supported in part by the AFIMEGQ project. AFIMEGQ (Africa For Innovation, Mobility, Exchange, Globalization and Quality) is a cooperation and mobility programme in the area of Higher Education, implemented by the Education, Audiovisual and Culture Executive Agency (EACEA) of the European Union (EU) and in part by the CSPT project (Special Standing Committee on Telecommunications) of Ministry of Higher Education of Morocco.

REFERENCES

1. ICNIRP, "Guidelines for limiting exposure to time-varying electric, magnetic and electromagnetic fields (up to 300 GHz)," *Health Physics*, Vol. 74, No. 4, 494, 522, 1998.
2. De Miguel-Bilbao, S., J. Garca, V. Ramos, and J. Blas, "Assessment of human body influence on exposure measurements of electric field in indoor enclosures," *Bioelectromagnetics*, Vol. 36, No. 2, 118–132, 2015.

3. De Miguel-Bilbao, S., V. Ramos, and J. Blas, "Assessment of polarization dependence of body shadow effect on dosimetry measurements in 2.4 GHz band," *Bioelectromagnetics*, Vol. 38, No. 4, 315–321, 2017.
4. Krzysztof, G., Z. Patryk, and K. Jolanta, "The role of the location of personal exposimeters on the human body in their use for assessing exposure to the electromagnetic field in the radiofrequency range 982450 MHz and compliance analysis: Evaluation by virtual measurements," *BioMed Research International*, Vol. 2015, 2015.
5. Iskra, S., R. McKenzie, and I. Cosic, "Monte carlo simulations of the electric field close to the body in realistic environments for application in personal radiofrequency dosimetry," *Radiation Protection Dosimetry*, Vol. 147, No. 4, 517, 2011.
6. Gallastegi, M., M. Guxens, A. Jim'enez-Zabala, I. Calvente, M. Fern'andez, L. Birks, B. Struchen, M. Vrijheid, M. Estarlich, M. F. Fern'andez, M. Torrent, F. Ballester, J. J. Aurrekoetxea, J. Ibarluzea, D. Guerra, J. Gonz'alez, M. Röösli, and L. Santa-Marina, "Characterisation of exposure to non-ionising electromagnetic fields in the spanish inma birth cohort: Study protocol," *BMC Public Health*, Vol. 16, No. 1, 167, 2016.
7. Cansiz, M., T. Abbasov, M. Bahattin Kurt, and A. Recai Celik, "Mapping of radio frequency electromagnetic field exposure levels in outdoor environment and comparing with reference levels for general public health," *J. Expos. Sci. Environ. Epidemiol.*, Original Article, Nov. 2016.
8. Neubauer, G., S. Cecil, W. Giczi, B. Petric, P. Preiner, J. Frhlich, and M. Rsli, "The association between exposure determined by radiofrequency personal exposimeters and human exposure: A simulation study," *Bioelectromagnetics*, Vol. 31, No. 7, 535–545, 2010.
9. Roblin, C. and A. Sibille, "Measurement of a body-worn triaxial sensor for electromagnetic field and exposure assessment," *2014 8th European Conference on Antennas and Propagation (EuCAP)*, 2631–2635, Apr. 2014.
10. Blas, J., F. A. Lago, P. Fernndez, R. M. Lorenzo, and E. J. Abril, "Potential exposure assessment errors associated with body-worn RF dosimeters," *Bioelectromagnetics*, Vol. 28, No. 7, 573–576, 2007.
11. Bahillo, A., J. Blas, P. Fernndez, R. M. Lorenzo, S. Mazuelas, and E. J. Abril, "E-field assessment errors associated with RF dosemeters for different angles of arrival," *Radiation Protection Dosimetry*, Vol. 132, No. 1, 51–56, 2008.
12. Iskra, S., R. McKenzie, and I. Cosic, "Personal, non-invasive dosimetry for radio-frequency human exposure assessment," *2007 29th Annual International Conference of the IEEE Engineering in Medicine and Biology Society*, 2319–2322, Aug. 2007.
13. Thielens, A., H. De Clercq, S. Agneessens, J. Lecoutere, L. Verloock, F. Declercq, G. Vermeeren, E. Tanghe, H. Rogier, R. Puers, L. Martens, and W. Joseph, "Personal distributed exposimeter for radio frequency exposure assessment in real environments," *Bioelectromagnetics*, Vol. 34, No. 7, 563–567, 2013.
14. Weiland, T., "A discretization method for the solution of maxwells equations for six-component fields," *Electronics and Communications AEU*, Vol. 31, No. 3, 116–120, 1977.
15. Clemens, M. and T. Weiland, "Discrete electromagnetism with the finite integration technique," *Progress In Electromagnetics Research*, Vol. 32, 65–87, 2001.
16. Petoussi-Henss, N., M. Zankl, U. Fill, and D. Regulla, "The GSF family of voxel phantoms," *Physics in Medicine and Biology*, Vol. 47, No. 1, 89, 2002.
17. Iskra, S., R. McKenzie, and I. Cosic, "Factors influencing uncertainty in measurement of electric fields close to the body in personal rf dosimetry," *Radiation Protection Dosimetry*, Vol. 140, No. 1, 25–33, 2010.
18. Kwate Kwate, R., B. Elmagroud, C. Taybi, D. Picard, and A. Ziyyat, "Interaction between human body and personal radiofrequency dosimeter: Effects of the metal plate presence," *Proc. IEEE 14th Edition of the Mediterranean Microwave Symposium MMS14*, Marrakech, Morocco, Dec. 12–14, 2014.

19. Kwate Kwate, R., B. Elmagroud, C. Taybi, V. Beauvois, Ch. Geuzaine, D. Picard, and A. Ziyyat, "On calibration of correction law for EMF measurement errors due to the proximity of the human body," *Proc. IEEE 15th edition of the Mediterranean Microwave Symposium MMS15*, 1–4, Lecce, Italy, 2015.
20. Elmagroud, B., R. Kwate Kwate, C. Taybi, D. Picard, and A. Ziyyat, "Electromagnetic exposure assessment for telecommunication equipements using RF dosimeter," *Proc. IEEE 2nd International Conference on Information Technology for Organizations Development, IT4OD-2016*, Fez, Morocco, 2016.